CHEMISTRY
A EUROPEAN JOURNAL

ChemPubSoc
Europe

DOI: 10.1002/chem.201204385

Coupling Photocatalysis and Redox Biocatalysis Toward Biocatalyzed Artificial Photosynthesis

Sahng Ha Lee, Jae Hong Kim, and Chan Beum Park*[a]

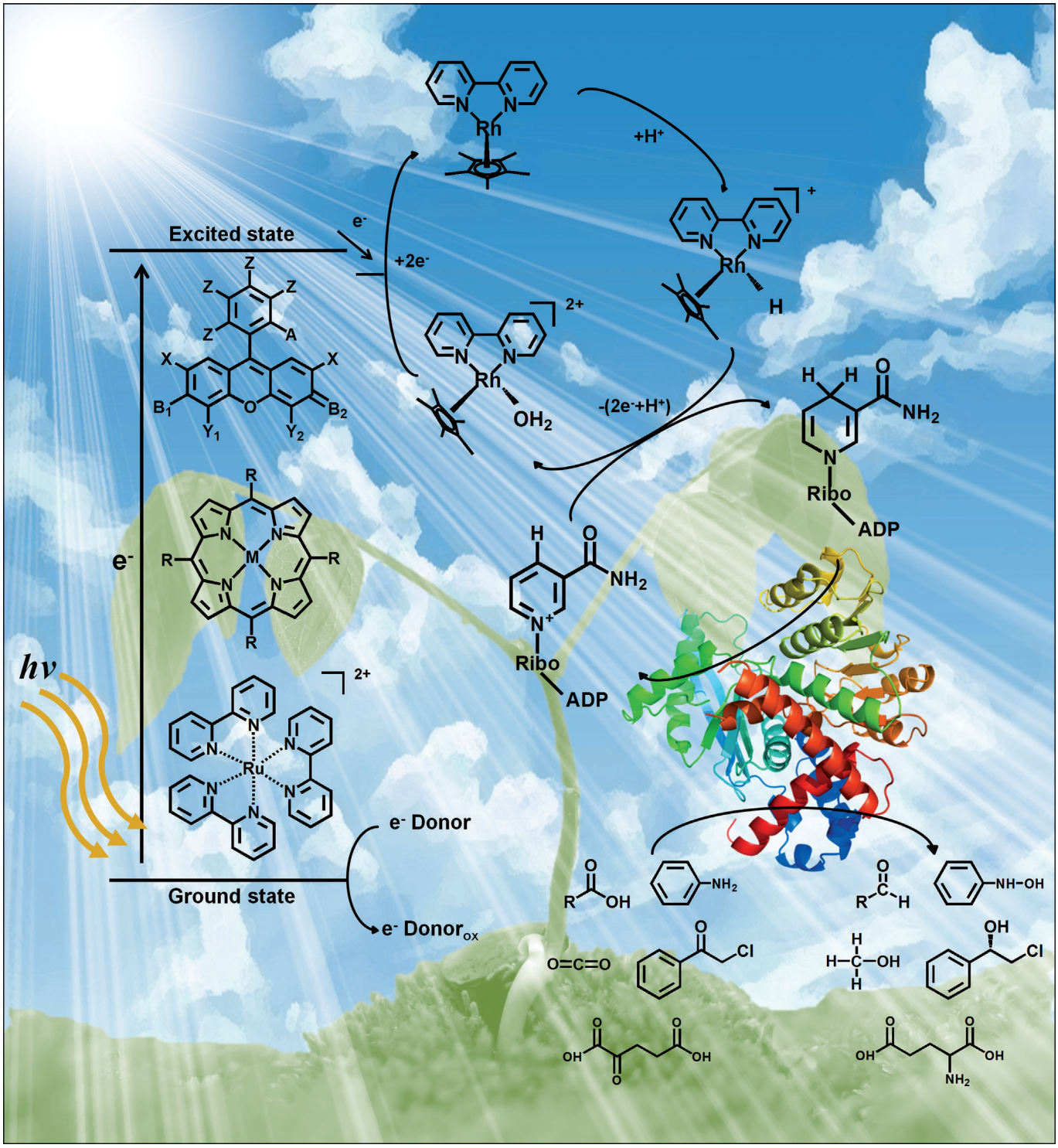

Abstract: In green plants, solar-energy utilization is accomplished through a cascade of photoinduced electron transfer, which remains a target model for realizing artificial photosynthesis. We introduce the concept of biocatalyzed artificial photosynthesis through coupling redox biocatalysis with photocatalysis to mimic natural photosynthesis based on visible-light-driven regeneration of enzyme cofactors. Key design principles for reaction components, such as electron donors, photosensitizers, and electron mediators, are described for artificial photosynthesis involving biocatalytic assemblies. Recent research outcomes that serve as a proof of the concept are summarized and current issues are discussed to provide a future perspective.

Keywords: biocatalysis · electron transport · photocatalysis · photosynthesis · redox chemistry

Introduction

Sunlight is the most abundant renewable-energy resource available on earth. The enormous energy of approximately 1.2×10^5 TW is delivered continuously from sun to earth, and exceeds the rate of human-energy consumption by 10^6 times.[1,2] Most solar energy, however, just passes through the earth by reflection or radiation, and less than 1% of the energy is utilized by activities on earth such as natural photosynthesis. The photosynthesis in green plants occurs through a complex cascade of photoinduced energy-transfer steps, mainly composed of light and dark reactions (also known as the Calvin cycle), as depicted in Scheme 1. The light reaction occurs through the Z-scheme, consisting of two photosystems (I and II) that contain an oxygen-evolving complex, light-harvesting antennae, and an electron-transport chain as key components. The sunlight collected by the light-harvesting antennae in photosystem II leads to the excitation of chlorophyll molecules (P680→P680*), which promotes the oxidation of water ($H_2O\rightarrow0.5\,O_2+2\,H^++2\,e^-$). The excited electrons from photosystem II are re-excited by the light-harvesting complex (P700→P700*) in photosystem I through the electron-transport chain. Ultimately, solar energy is stored in energy-rich biomolecules, such as ATP and NAD(P)H cofactors, as a result of photosensitized reactions through a cascade of wireless electron transfers. The cofactors further work as a reducing chemical for the reduction of CO_2 to carbohydrates through a series of light-independent, redox enzymatic reactions in the Calvin cycle. The natural photosynthesis through the Z-Scheme serves as an elegant example of how a fine nexus between photocatalysis and biocatalysis could be designed.[3]

The unique features (e.g., near-unity quantum yield and environmental compatibility) of natural photosynthesis have fascinated scientists in the past decades, and many efforts have been devoted to imitating the photovoltaic effect in nature. Thus, the utilization of solar energy, through photoinduced electron transfer, remains a target model for the development of artificial photosynthetic systems that utilize solar light as a sustainable and environmentally benign energy source.[4–7] The conversion of photon energy into electricity has been realized by the development of solar cells; in particular, the very concept of dye sensitization in natural photosynthesis is mimicked by dye-sensitized solar cells (DSSCs) that operate with an association of light-absorbing photosensitizers and charge-separating matrices. For artificial photosynthesis, a photoinduced electron-transfer reaction should occur through a man-made, light-harvesting photosensitizer in the presence of electron donors and acceptors, which can fulfill the role of both photosystems in

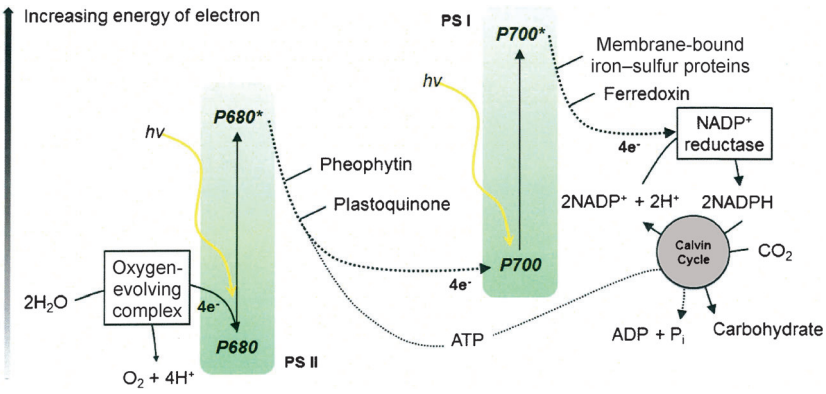

Scheme 1. Schematic illustration of natural photosynthetic pathway with light reaction (Z-Scheme) and dark reaction (Calvin cycle). During the photosynthetic process, photon energy is absorbed by dye-sensitized photosystems (i.e., PS II and I), and the electrons generated from water oxidation by the oxygen-evolving complex are transferred to $NADP^+$ reductase by means of an electron-transport chain comprised of pheophytin, plastoquinone, membrane-bound iron–sulfur proteins, and Ferredoxin. The excited electrons were used to regenerate NADPH and ATP for the reduction of carbon dioxide to carbohydrate in the Calvin cycle.

[a] S. H. Lee,[+] J. H. Kim,[+] Prof. C. B. Park
Department of Materials Science and Engineering
Korea Advanced Institute of Science and Technology (KAIST)
335 Science Road, Daejeon 305-701 (Republic of Korea)
Fax: (+82) 42-350-3310
E-mail: parkcb@kaist.ac.kr

[+] These authors contributed equally to this work.

natural photosynthesis.[5,8] Conventional approaches in artificial photosynthesis focus mainly on how to make a photoinduced electron-transfer reaction more efficient, and the final destination of photoexcited electrons is often limited to fuel production (e.g., H_2 or CH_3OH). While natural photosystems hint at the design of solar-energy storage in connection to enzymatic catalysis, they are too complex to be directly coupled with synthetic biocatalysis. Biocatalyzed artificial photosynthesis attempts the construction of a photobioreactor system that mimics the synthetic part of natural photosynthesis through an integral coupling of photocatalysis and biocatalysis cycles, with the ultimate goal of utilizing solar energy for the synthesis of fine chemicals and fuels, as depicted in Scheme 2. This process is accomplished by visible-light-driven regeneration of biochemical cofactors, such as NAD(P)H, through photosensitization by organic dyes or inorganic semiconductors. The excited electrons generated by the photosensitization are stored in the form of NAD(P)H and the reducing power is consumed during redox enzymatic reactions.

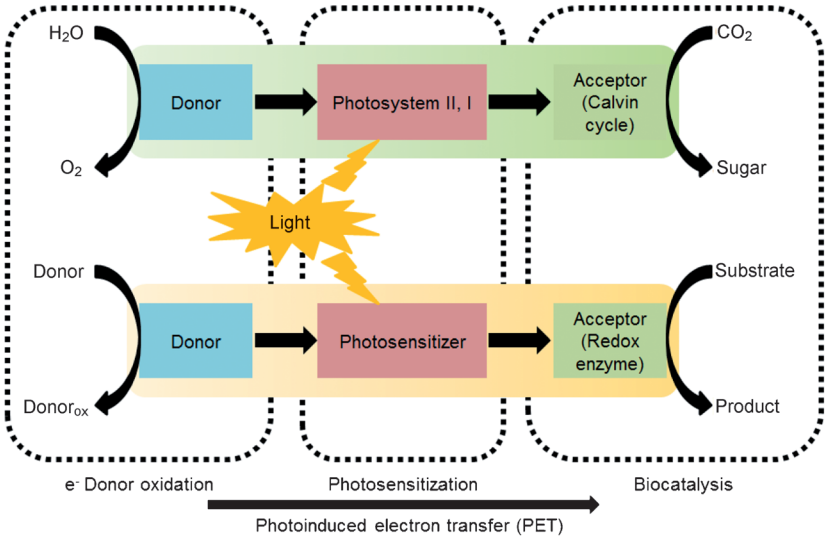

Scheme 2. Visible-light-driven chemical synthesis in natural photosynthesis and biocatalyzed artificial photosynthesis. In a simplified view, the D(donor)–P(photosensitizer)–A(acceptor) assembly in natural photosynthesis is composed of a water-splitting catalyst as the donor, photosystems as the photosensitizer, and the Calvin cycle as the acceptor. In biocatalyzed artificial photosynthesis, the natural photosystems (II and I) are replaced by man-made photosensitizers. Finally, the synthetic part of the photosynthetic system is replaced by redox enzymatic reactions.

Redox enzymes (or oxidoreductases) can catalyze highly sophisticated reactions that conventional chemical catalysts are unable to catalyze.[9] Despite their potential in complex organic synthesis, they often require the supply of a stoichiometric amount of expensive cofactors that have two contrary states (i.e., oxidized vs. reduced) for their catalytic activities. Thus far, numerous efforts have been made in the development of in situ regeneration of cofactors from its consumed counterpart toward the practical application of oxidoreductases in the biocatalytic industry.[10,11] While conventional cofactor regeneration methods, such as the use of a secondary enzyme, have the drawbacks of biocatalyst instability, low specific activity, and limited applications,[9,12] photochemical cofactor regeneration in biocatalyzed artificial photosynthesis provides an opportunity to utilize clean and abundant solar energy by mimicking natural photosynthesis. In photochemical cofactor regeneration, the electron-transfer cascade is initialized by photosensitization, and the excited electrons in the photosensitizer are transferred to the electron mediator, while electron donors compensate for the electron depletion in the photosensitizer, as illustrated in Scheme 3. The reduced mediators then reduce cofactors to drive the biocatalytic reaction with redox enzymes. In this article, we describe the concept of about how to design the key components of biocatalyzed artificial photosynthesis,

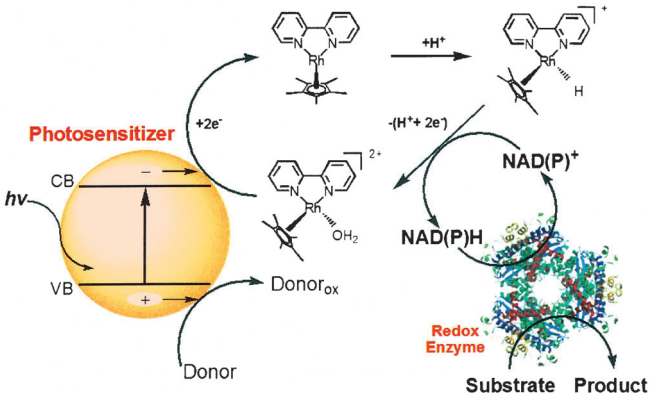

Scheme 3. Photoinduced electron transfer in biocatalyzed artificial photosynthesis through a cascade comprised of an electron donor, photosensitizer, Rh-based electron mediator (**M**), nicotinamide cofactor, and redox enzyme.

such as electron donors, photosensitizers, and electron mediators for photoinduced electron transfer and cofactor regeneration. While artificial photosynthesis using biocatalytic assemblies hints at the utilization of solar energy through coupling photocatalysis and enzymatic catalysis, the technology is still in its infancy and there remain many challenges to address that will be discussed as future perspectives.

Electron Donors and Mediators

Electron donors: For sustainable photosynthesis, an electron donor should provide electrons continuously to the ground state of a photosensitizer (Scheme 4, Path I). In natural pho-

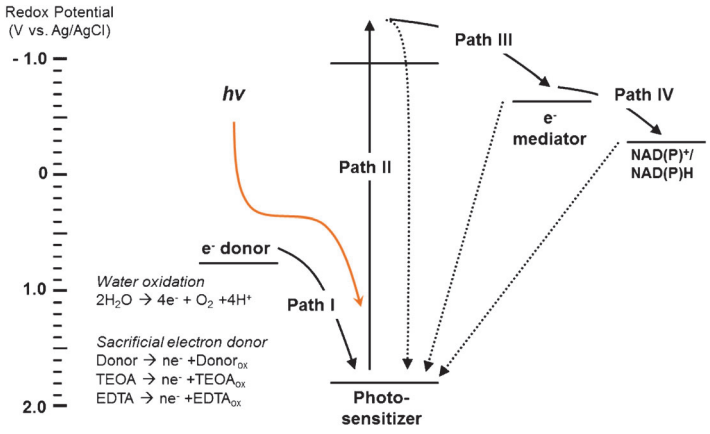

Scheme 4. Possible pathways of electron flow during biocatalyzed artificial photosynthesis. Electrons from the oxidation of water or sacrificial reagents (Path I) are excited by the photosensitizer (Path II) and transferred to an electron mediator or quenched to the ground state (Path III). The regeneration of NAD(P)H (Path IV) occurs through a gradient of electrochemical potential between the electron mediator and $NAD(P)^+$.

tosystem II, a calcium–manganese ($CaMn_4O_5$)-based complex supplies multiple electrons to chlorophyll through water oxidation.[13–15] High-density photon flux is critically needed for water splitting; four electrons are extracted rapidly by chlorophyll to form one oxygen molecule from the oxidation of two water molecules.[16] The $CaMn_4O_5$-based complex and light-harvesting antennae quickly transfer the four electrons obtained from the water splitting to the electron-transfer chain, composed of pheophytin and plastoquinone. In artificial photosynthesis, man-made photosensitizers, such as organic dyes and semiconductor nanomaterials, are employed to absorb photons as like chlorophyll in natural photosynthesis. To utilize water as an electron donor, cocatalysts that can play the role of the $CaMn_4O_5$-based complex in photosystem II are required, because most photosensitizers are incapable of catalyzing the rearrangement of water molecules to produce oxygen. Thus far, many researchers have made efforts to develop efficient water oxidation catalysts that can mimic the oxygen-evolving complex in nature. For example, metal oxide nanoparticles (e.g., IrO_2, Co_3O_4, Mn_2O_3, and Fe_2O_3), metal-containing complexes (e.g., cobalt-phosphates (Co-P_i) and polyoxometalates), and molecular catalysts containing a single metal (e.g., cobalt, iridium, ruthenium, and manganese) have been tested for the acceleration of the rate of water oxidation.[17–22] However, the oxygen evolution rates obtained with these catalysts are still much lower than those obtained with photosystem II in green plants (turnover frequency ca. 25 s^{-1}). The density of electron transfer from water oxidation is often insufficient, because of the loss of photoexcited electrons by back-electron transfer.

Due to the difficulties in using water as an electron donor, most studies in biocatalyzed photosynthesis have involved organic sacrificial agents such as triethanolamine (TEOA), triethylamine (TEA), ethylenediaminetetraacetic acid (EDTA), and ascorbic acid. These sacrificial electron donors can facilitate efficient electron transfer to a photosensitizer, because only transfer of a single electron is needed for the oxidation of an electron donor, while water oxidation is based on four-electron transfer. In addition, TEOA and TEA can coordinate easily with organic dyes (e.g., metal-containing polypyridine or porphyrin complexes) by means of noncovalent interactions (e.g., axial ligation) between the metal center in organic dyes and the nitrogen atom in TEOA and TEA.[23,24] Such interactions prevent nonproductive, back-electron transfer from the electron mediator (or cofactor) to the photosensitizer, indicated by the dotted arrows in Scheme 4. The decrease of back-electron transfer originates from the transformation of an intramolecular electron transfer to an inner-sphere one. Thus, organic electron donors can efficiently supply electrons to photosensitizers, and the overall reaction is often thermodynamically downhill. However, the accumulation of an oxidized form, consisting primarily of useless chemicals, remains a challenge in the development of a sustainable photosynthetic system; for example, the oxidation of TEOA (E_{ox} ca. 0.673 V) and EDTA (E_{ox} ca. −0.017 V) yields glycolaldehyde and formaldehyde, respectively.[25,26]

Electron mediators: Electron mediators obtain electrons from high-energy electron sources (i.e., photosensitizers), as indicated in Scheme 4 (Path III). In natural photosystems, high-energy electrons are transferred through an electron-transport chain and finally reduce ferredoxin, an iron–sulfur protein. Ferredoxin, acting as an electron-transfer mediator, reacts with ferredoxin–NADP reductase (FNR) to regenerate enzymatically active nicotinamide cofactors. Previously, electron mediators, such as methyl viologen, a highly toxic chemical, had been used for cofactor regeneration coupled directly with enzymes (e.g., diaphorase, lipoamide dehydrogenase, and FNR), as illustrated in Scheme 5.[27,28] In these systems, electron mediators are photochemically reduced by photosensitizers and work as an electron shuttle for redox enzymes that provide catalytic activity to regenerate cofactors in an enzymatically active form. Thus, a redox enzyme that is coupled with the electron mediator works as a catalytic assembly for photochemical regeneration of cofactors. In the absence of enzymatic mediation, a direct electron transfer from these mediators to the cofactors would occur, decreasing the specificity and selectivity in the cofactor regeneration. Such direct reduction induces the formation of isomers and dimers of reduced nicotinamide cofactors that are not suitable for the dark reaction of redox enzymatic synthesis.[29]

The use of a single regeneration catalyst is rather desirable for resolving the inherent short comings, such as the biocatalyst requirement as well as instability and separation problems of enzyme-mediated cofactor regeneration.[30,31] For non-enzymatic regeneration of nicotinamide cofactors, electron mediators should fulfill the following requirements:[32] 1) transfer of two electrons at once to prevent the formation of cofactor radicals and 2) generation of 1,4-

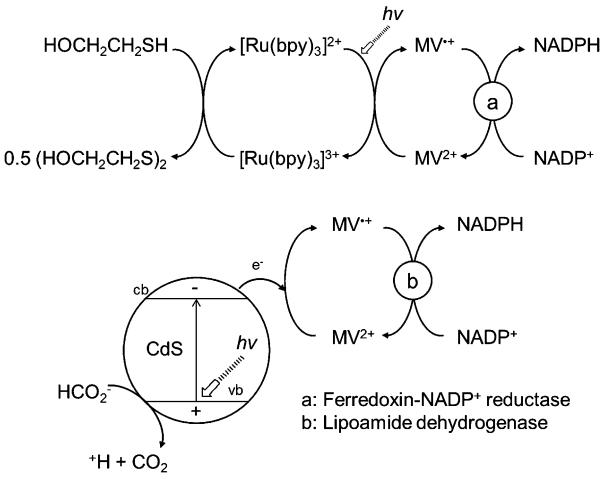

Scheme 5. Biocatalyzed artificial photosynthesis using methyl viologen (MV) coupled directly with enzymes (e.g., ferredoxin-$NADP^+$ reductase and lipoamide dehydrogenase) for nicotinamide cofactor regeneration. Photoexcited electrons in $[Ru(bpy)_3]^{2+}$ or CdS are transferred to methyl viologen, which is used for the enzymatic regeneration of NADPH. Mercaptoethanol and formate were used to scavenge the loss of electrons in the photosensitizers. Reproduced with permission from references [27,28].

NAD(P)H by a region-selective reaction. A rhodium-based organometallic mediator, $[Rh(bpy)(Cp^*)H_2O]^{2+}$ (**M**; bpy = bipyridine, Cp* = pentamethylcyclodienyl), developed by Steckhan and co-workers[33–35] has been most widely utilized for non-enzymatic cofactor regeneration, because **M** exhibits high robustness in terms of stability over pH and temperature, while also satisfying the two requirements noted above.[35,36] The oxidized form of **M** is reduced by taking two electrons and one proton, and the reduced form of **M** ($[Rh(bpy)(Cp^*)H]^+$), which is a hydride-carrying intermediate, transfers hydride to $NAD(P)^+$ through its coordination with the carbonyl-O atom in the pyridine ring of $NAD(P)^+$.[37,38] Because of the versatility of **M** for different cofactors and prosthetic groups (e.g., $NAD(P)^+$, flavins, and heme) of redox enzymes, it has been applied to nonconventional cofactor regeneration through chemical, electrochemical, and photochemical routes.

Because of the unique features of **M**, its analogues were synthesized for more versatile and efficient application to NAD(P)H cofactor regeneration.[39,40] For example, a series of [Rh(bpy)(Cp*)] analogues was synthesized through the modification of the bipyridine group with hydroxyl, carboxyl, amine, and methyl functional groups.[39] The reduction potentials of [Rh(bpy)(Cp*)] analogues are affected by the electrochemical properties of the substituting functional group, which results in cathodic and anodic shifts of the potentials. The substitution by electron-withdrawing groups (e.g., the carboxylic group) induces an anodic shift of reduction potential, making it easier to be reduced cathodically, while the substitution by electron-donating groups (e.g., amine and methyl groups) induces cathodic shifts. The turnover frequency of the modified catalyst was enhanced approximately three times more than that with methyl substitution, although not all of the [Rh(bpy)(Cp*)] analogues are catalytically active for NAD(P)H regeneration. In addition, phenanthroline (Phen) complexes based on rhodium, iridium, and ruthenium (e.g., [Rh(Phen)(Cp*)], [Ir(Phen)(Cp*)], and [Ru(Phen)(Cp*)]) were synthesized for formate-driven chemical regeneration of NADH.[40] The turnover frequency increased twice ($2000\ h^{-1}$) compared with the bipyridine-based complex, which suggests that the efficiency of **M** can be enhanced with proper modifications.

Cofactors: Nicotinamide cofactor is a key biological electron mediator required for many biocatalytic oxidation–reduction reactions. The reduced form of nicotinamide cofactors (i.e., NAD(P)H) enables redox enzymes to catalyze diverse and useful reactions, such as hydroxylation, epoxidation, Baeyer–Villiger reaction, and CO_2 reduction.[30,41–45] The electrochemical reduction of $NAD(P)^+$ into NAD(P)H occurs through a two-step electron transfer from an electron donor, followed by protonation.[46] The electron-transfer stpes occur at −1.1 and −1.7 V (vs. SCE). Due to the stepwise, multi-electron reaction, an intermediate state of reduced NAD(P) exists as a radical form (i.e., $NAD(P)^{\bullet}$) after the primary reduction reaction. The secondary reduction and protonation steps generate several isomers of reduced NAD(P)H (e.g., 1,4-NAD(P)H, 1,2-NAD(P)H, and 1,6-NAD(P)H). In addition, NAD radicals react together and produce dimers ($NAD(P)_2$) as a side reaction.[30,36] In order to avoid the formation of NAD(P)H isomers and dimers, which are enzymatically inactive, except for 1,4-NAD(P)H, the utilization of an enzyme or regiospecific electron mediator (e.g., **M**) is unavoidable, thus complicating photo- or electrochemical NAD(P)H regeneration.

The low stability of NAD(P)H in an aqueous medium also poses an obstacle for sustainable photoenzymatic synthesis. NAD(P)H decomposes under neutral and acidic conditions at ambient temperatures.[47] For example, only 5% of active NADH remains after 24 hour incubation at 37 °C.[48] NAD(P)H decomposition occurs through general acid-catalyzed protonation at the C-5 position of the nicotinamide ring, followed by nucleophilic attack on the C-6 position of the resulting imine.[49–51] The rate of NADH decomposition accelerates with the increasing temperature.[48] Thus, it is necessary to maximize the turnover rate of NAD(P)H regeneration, while maintaining a minimal cofactor concentration and a low temperature for a cost-efficient photoenzymatic process. The use of cofactor analogues with different spectral and redox properties from NAD has been attempted to avoid such problems as cofactor instability and to enhance regeneration efficiency.[48,52] In a recent study,[52] NAD analogues with different functionalities at their 3-substituted pyridine ring were examined as potential substitutes of NAD for eosin Y-sensitized photoenzymatic reactions; for example, nicotinamide adenine dinucleotide (NAD, R = $CONH_2$), 3-acetylpyridine adenine dinucleotide (APAD, R = $COCH_3$), 3-pyridinealdehyde adenine dinucleotide (PAAD, R = CHO), thionicotinamide adenine dinucleotide (TNAD, R = $CSNH_2$), and nicotinic acid adenine dinucleo-

tide (NAAD, R = COOH). Among the analogues, APAD displayed the fastest reduction rate as an artificial electron carrier and the reduction yield was in the order of APAD > PAAD > NAD > TNAD > NAAD. The electrochemical property of each cofactor was affected by the functional group substitution and the reduction potential became lower in the order of APAD < PAAD < NAD < TNAD < NAAD, which indicates that the cofactors with lower reduction potential show higher reduction yield. Furthermore, the stabilities of APADH and PAADH were found to be much higher than that of NADH at ambient temperatures.

While natural photosynthesis relies on nicotinamide cofactors as a reducing power, flavin-based molecules, such as flavin adenine dinucleotide (FAD) and flavin mononucleotide (FMN), are another class of key biological cofactors that work as a redox center for many oxidoreductases. For example, flavin-dependent monooxygenases (or flavoenzymes) contain enzyme-bound flavin cofactors, which have been studied extensively because of their capacity for driving a wide variety of redox reactions, such as regioselective hydroxylations and enantioselective sulfoxidation reactions.[53] The reduction of FAD into $FADH_2$, a hydroxyquinone, occurs through the uptake of two electrons and two protons,[54] which work as an active site (or electron source) for flavoenzymes either by activating molecular oxygen or by providing electrons to the active site of flavoenzymes.[55,56] The first step in the electrochemical reduction of FAD is observed at around −0.42 V (vs. SCE),[57] which is much higher than that of NAD (−1.1 V vs. SCE). In flavoenzyme-catalyzed reduction reactions, NAD(P)H can donate two electrons required for the reduction of enzyme-bound FAD (Scheme 6A).[58] Flavin cofactors themselves exhibit strong visible-light absorption and can also work as photosensitizers for the regeneration of flavoenzymes.[59] In the absence of the nicotinamide cofactor, photoexcited FAD molecules can react with enzyme-bound FAD to enable biocatalytic reactions, as illustrated in Scheme 6B.[58] Several research groups reported that the prosthetic groups in Baeyer–Villiger monooxygenases and cytochrome P450s can be regenerated through the direct (or indirect) photochemical reduction of external flavins (e.g., FAD, FMN, and riboflavin) that donate electrons to the enzyme-bound FAD.[59–61] Also, according to a recent report,[62] the generation of activated oxygen (e.g., H_2O_2) by the photosensitization of flavin molecules enabled photobiocatalytic oxyfunctionalization reactions (e.g., hydroxylation and epoxidation) driven by an aromatic peroxygenase, which showed superior and robust activities compared with chloroperoxidase.

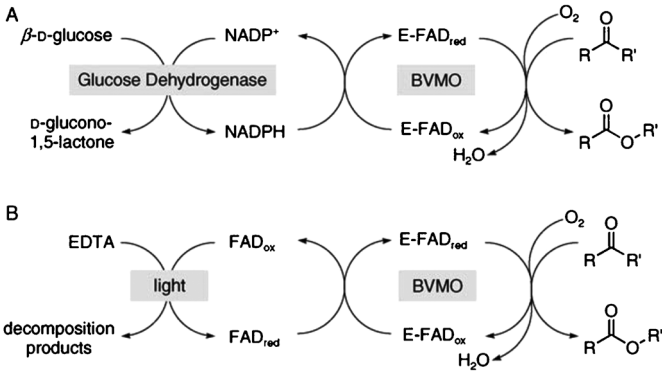

Scheme 6. Comparison of A) a conventional Baeyer–Villiger monooxygenase (BVMO, for example, PAMO) regeneration through enzymatic regeneration of NADPH and B) a light-driven pathway using photosensitization of an external flavin molecule. The enzyme-coupled system employs glucose dehydrogenase to regenerate reduced nicotinamide cofactor. The enzyme-coupled reaction can be replaced by a visible-light-driven redox reaction, reducing the complexity of the setup by eliminating the need for a coupled enzyme. E-FAD: enzyme bound flavin adenine dinucleotide. Adapted from reference [58].

Rational Design of Photosensitizers for Photoinduced Electron Transfer

Photoinduced electron transfer (PET) is a key mechanism that enables light-initiated cascade reactions for solar-energy conversion in natural photosynthesis.[63] In PET, light absorption by photosensitizers produces photoexcited electrons, followed by charge separation through a redox-mediating electron-transport system.[64] Upon the absorption of light, the internal energy state of a photosensitizer undergoes an electronic transition from a ground state (HOMO, valence band) to an excited state (LUMO, conduction band). Unless the electrons in the excited state are transferred to another electron-accepting molecule, they return to the ground state by emitting the absorbed energy through fluorescence.[65] Photosensitizers have been widely used for various photochemical applications, such as biomedical imaging, photodynamic therapy, DSSCs, and solar fuel production,[66–70] and rational design and engineering of photosensitizing materials is critical for the development of an artificial photosynthetic process. The performance of a photosynthetic reaction is primarily dependent on the light-conversion efficiency (e.g., turnover frequency and quantum yield) of a photosensitizer.[71] Furthermore, a proper electron-transport chain should be constructed to complete the PET system.[72] Since the photochemical regeneration of cofactors in biocatalyzed artificial photosynthesis occurs through a chain reaction (electron donor→photosensitizer→electron mediator→cofactor), the interaction between photosensitizer and electron mediator should meet the following conditions for successful regeneration of cofactors under visible light:

1) Existence of a proper energy-transfer relationship (e.g., fluorescence quenching) between the photosensitizer and electron mediator.
2) Higher energy level of the excited electrons of the photosensitizer than the reduction potential of the electron mediator (e.g., $E_{\mathbf{M}} = -0.75$ V vs. $Ag/AgCl_{3M\,NaCl}$, pH 7.0).
3) Attractive interactions between the photosensitizer and electron mediator (e.g., electrostatic interactions between organic dyes and **M**).

Different types of photosensitizers, such as organic dyes (e.g., xanthenes, porphyrins, and dye/graphene hybrid) and inorganic semiconductors (e.g., quantum dots, doped TiO_2, and silicon nanowires), have been applied thus far to biocatalyzed artificial photosynthesis, as summarized below.

Organic dyes: Xanthene dyes shown in Scheme 7A absorb visible light in the range of 500–600 nm to generate photoexcited electrons by an internal singlet–triplet transition.[73,74] They have been applied to DSSCs, photochemical hydrogen production, and cell imaging.[75–77] Recently, xanthene dyes have been utilized for biocatalyzed artificial photosynthesis as a molecular photoelectrode that produces photoexcited electrons upon visible-light irradiation.[78,79] The efficiency of photoenzymatic synthesis was significantly influenced by the structures of the dye molecules, which determine the electrochemical properties of the dyes and their interaction with **M**. Among many xanthene dyes, fluorescein and its halogenated derivatives (e.g., eosin Y, erythrosine B, rose bengal, and phloxine B) enabled the coupling of photoexcited electrons with **M** to regenerate 1,4-NAD(P)H under visible light with high turnover frequencies. For example, the turnover frequency of eosin Y for NADH photoregeneration was 1690 h^{-1} at its maximum (Table 1). It was suggested that the carboxyl group of eosin Y binds with the metal center of **M** (Rh^{2+}) through ionic affinity to form a photosensitizer-mediator dyad (Scheme 7C). An efficient transfer of electrons occurred for the regeneration of NADH through a PET cycle originating from the vicinity and potential gradient between eosin Y and **M**. The substitution of the hydrogen atom in fluorescein by Br and I resulted in stronger electronegativity and higher cofactor regeneration efficiency [fluorescein (H) < eosin Y (Br) < erythrosine B (I)]. The xanthene dyes with the carboxyl group and hydroxyl group (e.g., eosin Y, rose bengal, and erythrosine B) facilitated the energy transfer when coupled with **M** according to fluorescence quenching, enabling more efficient cofactor regeneration. However, the fluorescence of rhodamine dyes (e.g., rhodamine B, rhodamine 6G, and sulforhodamine B), which have a positively charged amine group, was not affected by the presence of **M**, and they exhibited no activity toward photochemical NADH regeneration. A recent paper reported visible-light-driven NADH regeneration with proflavine, an acridine derivative functionalized with diamine.[80] Despite the absence of strong affinity with **M**, proflavine showed moderate, but approximately 13 times lower turnover frequency than that of eosin Y in photochemical NADH regeneration.

In nature, chlorophyll P700 acts as a light-harvesting molecule to generate photoexcited electrons that are provided from a water-evolving center. Chlorophyll P700 is a porphyrin composed of four pyrrole rings interconnected by methine bridges, and it exhibits high absorbance in the range of visible light (Soret band: 20000–400000 $M^{-1}cm^{-1}$ from 380 to 400 nm; Q-band: 10000–20000 $M^{-1}cm^{-1}$ from 500 to 600 nm). Inspired by the natural light-harvesting system, many researchers have attempted to utilize porphyrin molecules (Scheme 7B) for DSSCs, photoelectrochemical cells,

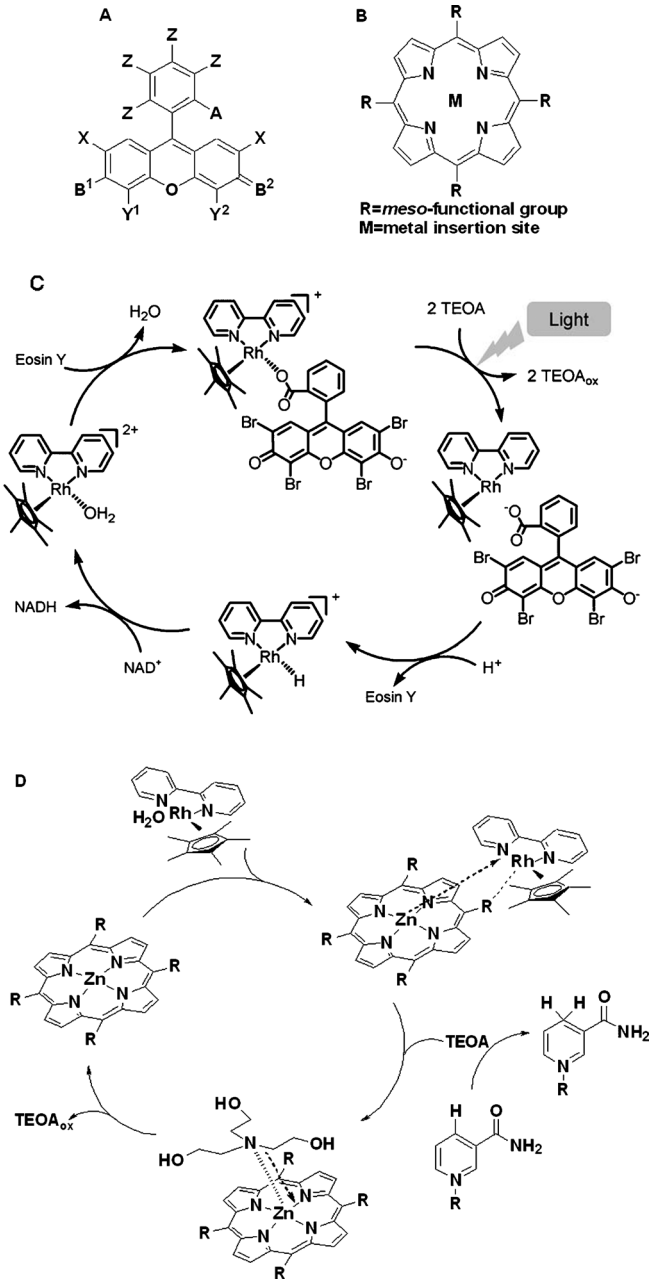

Scheme 7. A) Molecular structures of xanthene dyes. Possible functionalization groups: A = COOH, COOEt, SO_3H; B^1 = OH, NHEt, $NHEt_2$, N^+Et_2; B^2 = O, NEt, NEt_2, N^+Et_2; X = H, Br, I, NO_2, CH_3; Y^1 = H, Br, I, HgOH; Y^2 = H, Br, I; Z = H, Cl, SO_3H. B) Molecular structures of porphyrins. M is a metal insertion site (e.g., no metal, Zn, or Mn) and R is a *meso*-functional group (e.g., sulfonato and carboxyl group). C) Catalytic cycle of eosin Y sensitized, non-enzymatic photochemical regeneration of NADH involving two electron-transfer reactions between **M** and eosin Y. D) Catalytic cycle of visible-light-driven regeneration of NADH with Zn-containing porphyrin as a photosensitizer. Adapted from references [78,83].

and solar hydrogen production.[81–83] In biocatalyzed artificial photosynthesis, among many porphyrin molecules that have different metal insertion sites and *meso*-functional groups, Zn-containing porphyrins demonstrated the highest yield for photochemical NADH regeneration (Table 1). As illustrated

Table 1. Turnover frequencies (TOF) of molecular or colloidal photosensitizers (PS) used in photochemical regeneration of nicotinamide cofactor and redox enzymatic synthesis under visible light.

Classification	Photo-sensitizer	Redox potential[a] (vs. NHE) E_{red}	E_{ox}	[PS] [mM]	[NAD] [mM]	[**M**] [mM]	TOF[b] [h^{-1}]	TOF[c] [h^{-1}]	Ref.
organic									
xanthene	eosin Y	−0.92	1.15	0.001	1	0.25	1690	n.a.	[78]
xanthene	eosin Y			0.02	0.05	0.25	n.a.	1177	[79]
xanthene	phloxine B	n.a.	n.a.	0.02	0.05	0.25	n.a.	1537	[79]
xanthene	erythrosin B	−0.93	1.03	0.02	0.05	0.25	n.a.	1144	[79]
xanthene	rose bengal	−0.96	0.89	0.02	0.05	0.25	n.a.	1270	[79]
porphyrin	ZnTPPS	−0.96	1.06	0.5	1	0.5	0.46	n.a.	[83]
porphyrin	ZnTPPS			0.5	1	0.5	n.a.	0.27	[83]
porphyrin	ZnTPPC	−0.96	0.99	0.5	1	0.5	n.a.	0.22	[83]
porphyrin	H_2TPPS	−0.92	1.23	0.5	1	0.5	n.a.	0.16	[83]
porphyrin	H_2TPPC	−0.86	n.a.	0.5	1	0.5	n.a.	0.19	[83]
others	PEG-chlorophyllide	n.a.	n.a.	0.022	3.2	2.5 U[d]	n.a.	1.26	[86]
others	proflavine	n.a.	n.a.	0.01	1	0.25	127.8	n.a.	[80]
inorganic									
semiconductor	CdTe NPs	−0.6	1.0	20	1	0.25	0.54	n.a.	[98]
semi-conductor	CdSe NPs	−0.5	1.3	20	1	0.25	0.168	n.a.	[98]
semiconductor	CdS NPs	−0.6	1.7	20	1	0.25	0.120	n.a.	[98]
semiconductor	$W_2Fe_4Ta_2O_{17}$	n.a.	n.a.	5 mg	0.2	0.1	0.37	n.a.	[95]
semiconductor	p-doped TiO_2	n.a.	n.a.	80 mg	0.2	0.2	0.003	n.a.	[94]
metal	Pt NPs	n.a.	n.a.	0.092	0.2	n.a.	0.108	n.a.	[96]

[a] The values for redox potentials are estimated from the literature.[124–126] [b] TOF of photosensitizers for NADH regeneration. [d] TOF of photosensitizers for redox enzymatic synthesis. [d] Electron mediator was ferredoxin-$NADP^+$ reductase.

in Scheme 7D, the electron-donating ability of porphyrin and the electron transfer between porphyrin and the electron donor facilitate the PET. Zn-containing porphyrins have higher electronegativity than others, such as protoporphyrins and Mn-containing porphyrins, and they can interact with TEOA, an electron donor, through axial ligation between the Zn atom of porphyrins and the nitrogen atom of TEOA. The axial coordination leads to an intramolecular charge transfer between photosensitizers and electron donors, preventing back-electron transfer. The turnover frequency of porphyrin molecules for photochemical NADH regeneration is lower than that of other organic photosensitizers (e.g., eosin Y), and is attributed to possible side reactions, such as the production of superoxide and singlet oxygen.[84] Despite the relatively low efficiency of porphyrins for photochemical NADH regeneration, porphyrins are promising candidates for artificial photosynthesis, because they possess the ability to extract electrons from water molecules in the presence of an artificial oxygen-evolving center, such as IrO_2.[82,85] To prevent side reactions and improve the efficiency of photoinduced electron transfer, porphyrin molecules need to be conjugated with an oxygen-evolving catalyst and electron mediator in the future. The conjugation of organic photosensitizers with biocompatible polymers could improve the photostability of photosensitizers as well. For example, chlorophyll conjugated with polyethylene glycol (i.e., PEG–chlorophyllide) showed higher photostability compared to the pristine chlorophyll upon visible-light illumination, and a visible-light-driven photosynthetic reaction with PEG–chlorophyllide continued over 60 h.[86]

Carbon-based nanomaterials, such as fullerene, carbon nanotubes, and graphene, have been employed to enhance the PET, because of their unique properties (e.g., high conductivity, easy chemical functionalization, and thermal stability).[87] Recently, graphene/porphyrin hybrid materials were applied to biocatalyzed artificial photosynthesis.[42,88] In the studies, graphene conjugated with multianthraquinone-substituted porphyrin (MAQSP) enhanced the efficiency of visible-light-driven NADH regeneration in comparison with pristine MAQSP and $W_2Fe_4Ta_2O_{17}$.[42] The higher photocatalytic activity originated from an accelerated rate of electron transfer from MAQSP to **M**, owing to the high-electron-carrier mobility of graphene. Graphene sheets with a high surface area serve as an electron reservoir from which transport of multiple electrons from MAQSP to **M** can be realized. According to density functional theory (DFT) calculations, the energy-level alignment between the conduction-band edges of graphene and the LUMO of MAQSP facilitates efficient transfer of electrons from MAQSP to graphene. It was suggested that the problem arising from the large Coulomb repulsion between the localized electrons of MAQSP is resolved by the junction with graphene to provide the delocalized nature of wave functions. Such high efficiency in cofactor regeneration by the MAQSP–graphene catalyst was recently coupled with biocatalyzed asymmetric reduction of acetophenones with alcohol dehydrogenase (Scheme 8).[88] The MAQSP–graphene catalyst enabled photochemical asymmetric reduction of acetophenones with high enantiomeric excess (ca. 82–99%).

Inorganic photosensitizers: Semiconducting materials have been widely studied for photocatalytic water splitting and

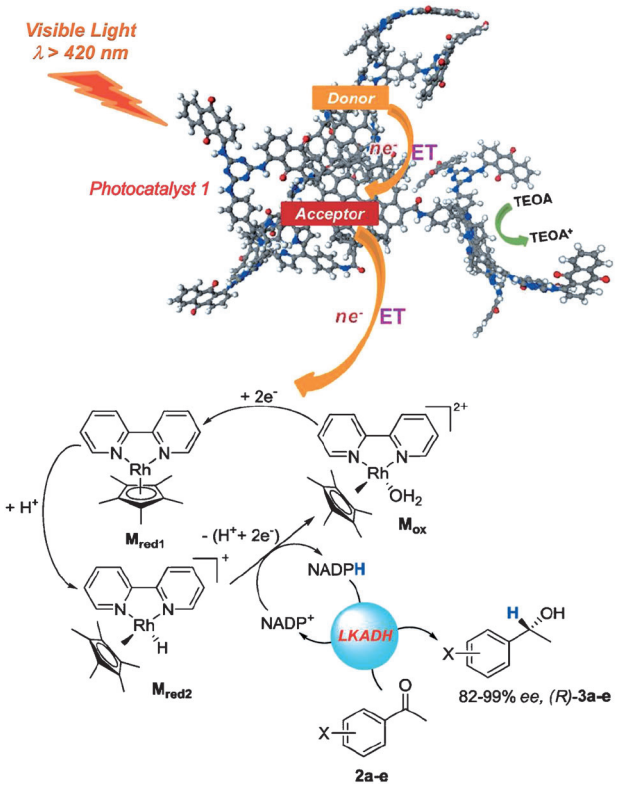

Scheme 8. Plausible mechanism of asymmetric reduction of acetophenones by alcohol dehydrogenase from Lactobacillus kefir (LKADH)/1,4-NADPH system under visible light (ET = electron transfer). Upon the absorption of visible light by graphene-conjugated MAQSP, the photoexcited electrons in MAQSP are separated by the graphene part of the photocatalyst. The electron transfer from the photocatalyst to **M** finally reduces $NADP^+$, which is subsequently used in the next step for the enzymatic asymmetric reduction of prochiral ketones. Adapted from reference [88].

solar H_2 production.[89,90] Many different types of semiconducting materials, such as metal oxides, quantum dots, and their composite materials, have been reported for heterogeneous photocatalytic reactions.[91] The electron-hole pairs formed within the photosensitized bandgap of semiconductors perform reduction–oxidation reactions when they are transferred to other molecules that function as electron acceptors or hole scavengers. Metal oxide semiconductor materials (e.g., TiO_2, WO_3, ZnO) are well-known photocatalysts with low cost, high efficiency, and good chemical inertness as well as stability, but their use as light-harvesting photosensitizers is often limited because of large optical bandgaps that make those materials inappropriate for applications under visible light. Compared with undoped metal oxides, doped metal oxide particles exhibit enhanced visible-light absorption and thus show much higher activity in NADH photoregeneration. For example, Jiang et al. applied TiO_2-based photocatalysts doped with carbon,[92] boron,[93] and phosphorus[94] for visible-light-driven NADH regeneration. The yield of NADH production was substantially enhanced by the increasing dopant proportion, indicating that the excited electrons could be separated by the surface traps arising from the doping. A composite semiconductor photocatalyst, such as $W_2Fe_4Ta_2O_{17}$, was also applied for photoenzymatic synthesis under visible light.[95] $W_2Fe_4Ta_2O_{17}$ promotes an electron to the conduction band upon band-gap excitation by visible light ($\lambda \geq 420$ nm). $W_2Fe_4Ta_2O_{17}$ showed turnover frequency of 0.37 h^{-1} for photochemical NADH regeneration and exhibited 3.7 times higher yield in L-glutamate dehydrogenase-catalyzed reduction of α-ketoglutarate when compared with N-doped TiO_2. In addition, it was reported that photochemical properties of colloidal Pt nanoparticles (NPs) could be applied to capture photons under visible light, so that the photoexcited electrons in the Pt nanoparticles would convert NAD^+ into NADH.[96] Colloidal photosensitizers, however, generally exhibit much lower molar efficiencies of photochemical cofactor regeneration in the order from 10^2 to 10^3 compared with molecular dyes (Table 1), because the photocatalytic process in inorganic, particulate photosensitizers involves internal diffusion of photoexcited electrons to the reactive surface, and this can cause charge recombination. The photocatalytic activity of inorganic photosensitizers may be improved by using nanosized semiconductors (e.g., quantum dots) and efficient charge separation methods such as heterojunction of photosensitizer-matrix materials.

The catalytic activities of semiconducting materials are influenced significantly by their size and structure, because surface properties, such as the state of metal ions on the surface at which the catalytic reactions occur, govern catalytic reactions. Nano-sized quantum dots have high surface-to-volume ratios and surface energy compared with bulk materials. They possess advantages of optical tunability due to the quantum-size-confinement effect and long-term stability over organic dyes.[97] In a recent study,[98] CdS, CdSe, and CdTe NP-based photochemical NADH regeneration was reported using the unique property of quantum dots as light-harvesting nanomaterial (Scheme 9 A). These quantum dots absorb incident light ($\lambda > 420$ nm) to generate excited electrons on conduction bands, and these electrons are then transferred to **M** for the regeneration of NADH. The photogenerated holes are scavenged by TEOA to sustain the visible-light-driven reaction. The regeneration efficiency was in order of CdTe > CdS > CdSe nanocrystals, but no photoreaction was observed with micron-sized CdS, CdSe, and CdTe, which indicates that NADH regeneration can be only achieved through the quantum effect and surface reactivity. The immobilization of quantum dots and redox enzymes on solid supports can further provide enhanced stability, repeated usability, and easy separation of photochemical reaction components. For example, micron-sized, SiO_2 bead-supported photoenzymatic synthesis was demonstrated through repeated cycles of NADH photoregeneration and redox enzymatic synthesis by using two different types of beads: CdS-coated beads for light reaction and enzyme-immobilized beads for dark reaction.[99]

Recently, a heterojunction photoelectrode consisting of CdS quantum dots and a TiO_2 nanotube array was devel-

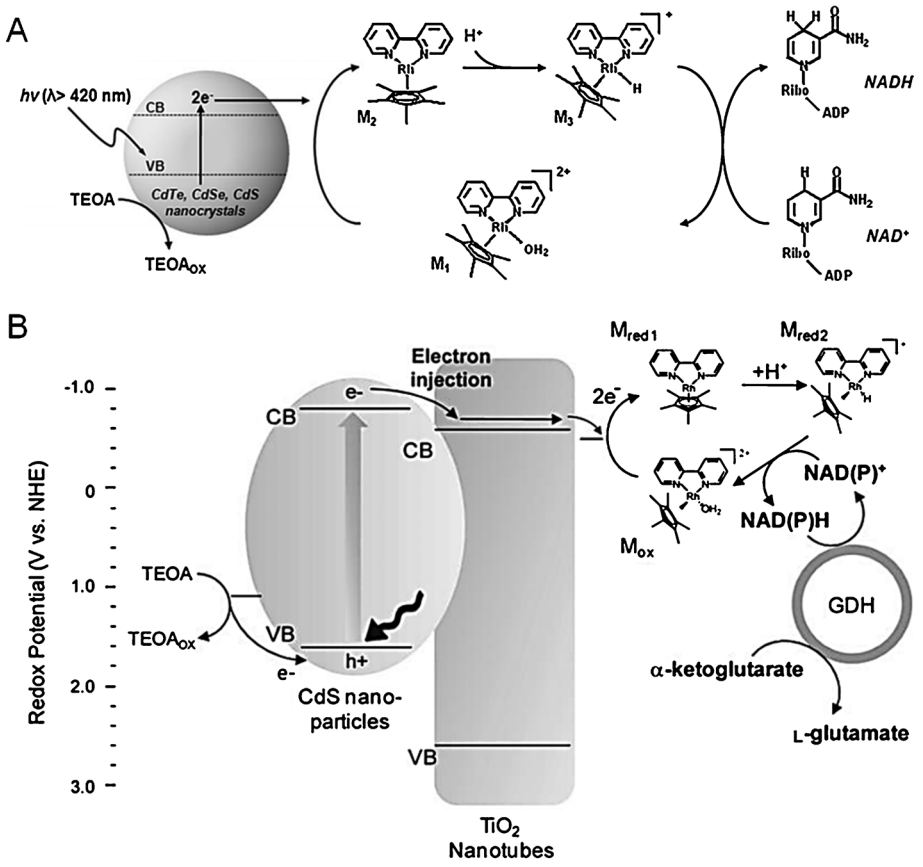

Scheme 9. Schematic diagrams of photochemical cofactor regeneration using inorganic photosensitizers. A) Regeneration of NADH by colloidal quantum dot nanocrystals (CdTe, CdSe, CdS). B) Photoenzymatic reaction through CdS-TiO_2 nanotube junction. Adapted from references [98, 100].

oped to imitate natural photosynthesis more closely.[100] The TiO_2–CdS nanotube array was made through reverse inspiration by the design of DSSC electrodes, which also mimic the reaction mechanism of natural photosynthesis. As described earlier, in natural photosynthesis, the excited electrons in chlorophyll are quickly transferred to an electron-transport chain before they return to their ground state. In a similar way, photoexcited electrons are efficiently separated by a heterojunction photoelectrode and transferred to an external wire for the generation of solar-powered electricity in DSSCs. As illustrated in Scheme 9B, a TiO_2–CdS heterojunction photoelectrode was utilized for biocatalyzed artificial photosynthesis to regenerate cofactors coupled with redox enzymatic catalysis (instead of electricity production in DSSCs). On the TiO_2–CdS nanotube array, photoexcited electrons are rapidly injected from the conduction band of CdS to the conduction band of nearby TiO_2 nanotubes under visible-light irradiation; this process generates reduction potential for NAD(P)H regeneration. Electrons are supplied from the oxidation of TEOA to the holes in the valence band of CdS NPs. TiO_2 nanotubes were prepared by using an electrochemical anodization, and the length and diameter of the TiO_2 nanotubes could be controlled through varying the anodizing conditions. The morphology of the TiO_2 nanotubes affected the entire photoreaction's efficiency significantly; the nanotubes with longer length and wider diameter resulted in a higher yield of NADH photoregeneration. The performance of photoreactions by the TiO_2–CdS nanotube array was also influenced by the crystallinity of TiO_2 nanotubes. Crystalline anatase TiO_2 nanotubes showed higher efficiency compared with amorphous TiO_2 nanotubes, because the lifetime of injected electrons becomes longer with higher crystallinity. In the case of Al_2O_3 nanotubes, an insulating material with an electron-uninjectable energy level, there was no electron-separation effect, resulting in an extremely low yield of NADH regeneration, owing to the high rate of charge recombination. When compared with TiO_2–CdS NPs, the nanotube array was more effective for photochemical reactions, because the higher aspect ratio of nanotubes provided a larger surface area that facilitated the diffusion of reactants. Taken together, efficient electron separation and diffusion by a heterojunction could be a useful strategy by which to design suitable photoelectrode materials for biocatalyzed artificial photosynthesis.

Another example of a photovoltaic material applied to biocatalyzed artificial photosynthesis is the silicon nanowire, which has many advantages for practical applications, such as low cost, high surface area, easy fabrication, and strong light absorption across the visible-light spectrum, unlike conventional semiconductor nanowires (e.g., TiO_2 and ZnO).[101–104] Recently, hydrogen-terminated silicon nanowires (H-SiNWs) were employed as an efficient photoelectrode for photoenzymatic synthesis under visible light (Scheme 10).[105] H-SiNWs, fabricated by a metal-assisted chemical etching process, possess an enlarged bandgap and enable a cascading electron transfer. The enlarged bandgap of H-SiNWs through the quantum-confinement effect triggered thermodynamically favorable electron transfer from electron donor to NAD^+ via **M**. Furthermore, the efficient PET from the H-SiNWs to **M** prevented the formation of an oxide layer (i.e., SiO_2) on the surface of the H-SiNWs. Hydrogen termination on the surface of silicon nanowires boosted the efficiency of photochemical NADH regeneration; approximately 80% of NADH was photoregenerated from NAD^+ by H-SiNWs within two hours of visible-light

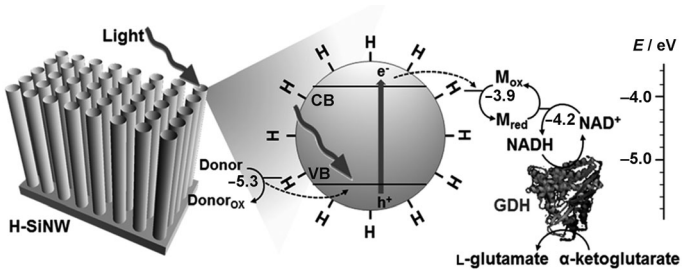

Scheme 10. Biocatalyzed artificial photosynthesis with hydrogen-terminated silicon nanowires (H-SiNWs) as a light-harvesting material. Under illumination of visible light ($\lambda > 420$ nm), excited electrons in the H-SiNWs are transferred to NAD^+ via the rhodium-based mediator (**M**), followed by biocatalytic conversion of α-ketoglutarate to L-glutamate. The hydrogen termination on the surface suppresses electron–hole pair recombination and aids efficient electron transfer to **M**. Adapted from reference [105].

irradiation, which was successfully coupled with redox enzymatic synthesis.

Integrated Platforms for Biocatalyzed Artificial Photosynthesis

Natural photosynthesis occurs in highly sophisticated nanostructures composed of chlorophyll aggregates, which serve as light-harvesting antennae, and catalytic metal clusters embedded within proteins. The interaction between chlorophyll aggregates induces the flow of excited electrons by Förster-type energy transfer.[106,107] The reaction center in the natural photosystem includes electron-donor and -acceptor assemblies, such as plastoquinone and tyrosine residues,[108,109] which facilitate energetically favorable electron transfer. Mimicking the structure of a natural photosystem is a good strategy for the development of an integrated platform for artificial photosynthesis. In the field of artificial photosynthesis, the integration of reaction components, such as the electron donor (D), photosensitizer (P), and electron acceptor (A), has been attempted by designing covalent, semicovalent, or noncovalent bonds between the components (i.e., D-P-A) on support materials to enhance the rate of electron transfer and photocatalytic efficiency.[110,111] Recently, virus-templated photocatalytic nanostructures were developed for sustainable water oxidation under visible light.[112] In this work, porphyrins and IrO_2 hydrosols were incorporated on the virus-templated nanowires as a photosensitizer and water oxidation catalyst, respectively. This assembly significantly enhanced the photocatalytic efficiency of water oxidation through efficient PET between the porphyrins and the IrO_2 hydrosols. Maeda et al. utilized niobate nanoscrolls and nanosheets as supporting materials for the assembly of $[Ru(bpy)_3]^{2+}$ and Pt.[113] The niobate nanoscrolls enhanced PET from $[Ru(bpy)_3]^{2+}$ to Pt, increasing the efficiency of hydrogen evolution under visible light. For biocatalyzed artificial photosynthesis, key components (e.g., D, P, A, cofactor, and enzyme) need to be incorporated into suitable support materials to maximize the confinement effect and the efficiency of PET, as well as to afford repeated usability. The supporting matrix can assist in the organization of the key photosynthetic components and protect them by providing a stable microenvironment.[114] Furthermore, this approach provides a means to readily handle photoactive materials and to facilitate recycling from the reaction mixture,[115] making the downstream process more simple and cost-effective.

In plant cells, crystalline cellulose microfibrils are linked to hemicelluloses to provide strength as well as extensibility, and lignin penetrates the in-between spaces, thereby conferring mechanical strength to cell walls.[116] Lee et al.[117] developed light-harvesting synthetic woods by encapsulating hydrophobic porphyrin molecules in a composite of three major structural components in plant cells: cellulose, hemicelluloses, and lignin. Synthetic wood, an all-wood composite, is environmentally friendly and highly desirable for replacing nonrenewable, petroleum-based synthetic polymers. Similar to the natural-light-harvesting by chloroplasts, porphyrin-encapsulated lignocellulosic hybrids harnessed visible-light-driven regeneration of a reducing power (i.e., NADH) for chemical synthesis catalyzed by NADH-dependent oxidoreductases. The turnover frequency of porphyrin encapsulated in synthetic wood was estimated to be approximately 1.25 h^{-1}. The synthetic wood not only provided a microenvironment for porphyrin encapsulation, but also facilitated an effective photosynthesis due to a redox-active lignin component. Free phenolic groups in lignin can undergo oxidation–reduction reactions by converting into electroactive quinine functionalities, which facilitate reversible proton-coupled two-electron redox cycling.[118,119] Thus, similar to the protein environment of the natural photosynthetic assemblies in the thylakoid membrane containing redox-active components, the local environment of the synthetic wood matrix composed of lignin assists with the charge transfer of encapsulated porphyrin for efficient biocatalytic photosynthesis.

Natural light-harvesting antennae, which are made through the self-assembly of chlorophyll molecules and proteins in photosynthetic units, are critically important for increasing the rate of PET.[120] Thus, many researchers have developed artificial light-harvesting antennae by means of self-assembly in order to improve the efficiency of artificial photosynthesis.[121] Recently, Kim et al. reported the synthesis of self-assembled, light-harvesting peptide nanotubes for a redox enzymatic reaction coupled with NADH regeneration under visible light.[122] The light-harvesting nanotubes were synthesized through the self-assembly of porphyrins and diphenylalanine (Phe–Phe, FF), a dipeptide consisting of two covalently-linked phenylalanine units. The carboxylic group of the self-assembled FF nanotubes provided sites for noncovalent interaction with the hydroxyl group of porphyrins. The immobilized porphyrins were arranged in an extended fashion on the surface of the peptide nanotubes, leading to exciton coupling between porphyrins, as in chlorophyll aggregates in natural photosystems. The electronic in-

teraction between porphyrins enhanced the efficiency of NADH regeneration in comparison with free porphyin monomers, because of the enhanced PET from the electron donor to NADH.

In addition to the spatial organization of photosynthetic platforms, microfluidic transport of fluids is a factor to be considered when trying to closely mimick natural photosynthesis that occur by enabling efficient transport of water and chemicals through microtube networks. Over the past decade, microfluidics has received considerable attention in diverse fields and can be a promising miniaturized platform for artificial photosynthesis, because it allows for improved energy density, sustainability, and recyclability. While a platform that enables the microfluidic transport of key chemicals for light-dependent and light-independent reactions is barely known, recently a microfluidic artificial photosynthetic system for in situ regeneration of reducing power (i.e., NADH cofactor) and redox enzymatic synthesis of chemicals under visible light has been reported (Scheme 11).[123] For the development of a photosynthetic microfluidic chip, microchannels were fabricated by using soft lithography and mold–eplica techniques, followed by covalent immobilization of a light-harvesting photosensitizer and redox enzyme in up- and downstream microfluidic zones, respectively. On the microfluidic platform, light-dependent and independent reactions take place simultaneously, as in the natural photosynthesis that occurs in the organelle of micron-sized chloroplasts containing light-harvesting thylakoid membranes. Both yields of light-induced NADH regeneration and photoenzymatic synthesis were highly affected by the retention time and light irradiation on the microfluidic platform. Furthermore, covalently immobilized quantum dots and redox enzymes within the separate microchannel zones allowed for repeated photoreactions under visible light. The photosynthetic microfluidic chip enables sustainable, integrated light-harvesting and photoenzymatic synthesis in a miniaturized architecture.

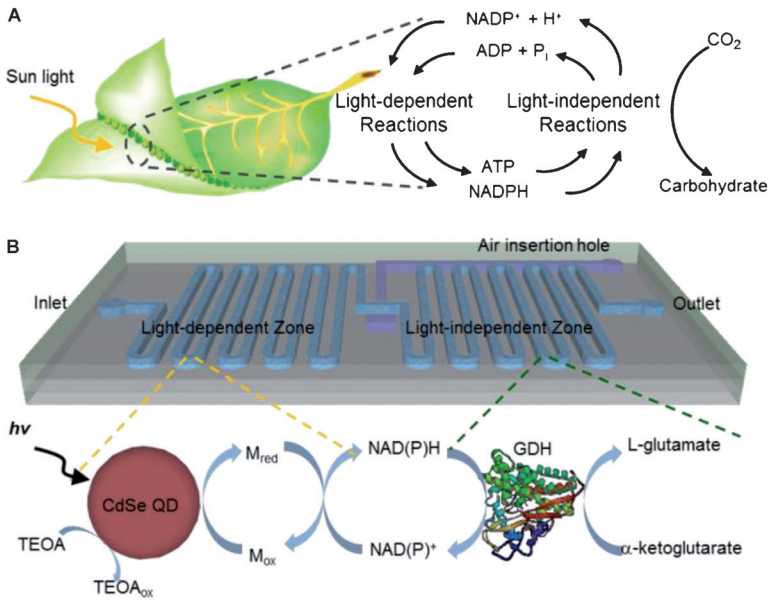

Scheme 11. Schematic illustrations for A) the natural photosynthesis in plants and B) a microfluidic artificial photosynthesis system. The microfluidic platform incorporates CdSe quantum dots and glutamate dehydrogenase (GDH) within separate microchannel zones. Similar to photosynthesis in green plants, light-driven nicotinamide cofactor regeneration takes place in the light-dependent reaction zone, which is then coupled with the light-independent, enzymatic synthesis of L-glutamate in the downstream of the microchannel. Adapted from reference [123].

Summary and Outlook

We have introduced the concept of biocatalyzed artificial photosynthesis that aims to graft solar-energy conversion with redox enzymatic catalysis by mimicking natural photosynthesis. In the past decades, the natural photosynthetic mechanism has provided much inspiration for the design of photovoltaics and photoelectrochemical cells. The artificial photosynthesis in biocatalytic assemblies has been recently demonstrated using organic (or inorganic) photosensitizers and redox enzymatic reactions through photochemical regeneration of biological electron mediators (e.g., nicotinamide and flavin cofactors). For the successful construction of photosynthetic system involving redox biocatalysts, it is critical to engineer key photochemical components, such as electron donors, photosensitizers, and electron mediators, for driving electron transport in the correct direction upon light irradiation. In nature, solar-energy utilization is accomplished through a complex chain of redox reactions in multiple photosystems under visible light and ambient conditions. Efficient electron transfer through a redox cascade from electron donor to cofactors is often thermodynamically unfavorable, resulting in back-electron transfer. Many additional features are needed for the realization of biocatalyzed artificial photosynthesis as follows:

1) Use of water as an electron donor (i.e., electron supply by water oxidation).
2) Efficient light-harvesting and PET.
3) Long-term stability of photosensitizers and electron mediators.
4) Reaction engineering to maximize photoenzymatic yields.
5) Integration of reaction system and design of cost-effective process.

In the future, it will be desirable to couple water oxidation with photoenzymatic synthesis through the development of ef-

ficient water-oxidation catalysts. Current use of organic sacrificial agents (e.g., TEOA) causes the accumulation of their oxidized form in the photochemical reaction system. To achieve visible-light-driven cofactor regeneration using water as an electron donor, the rate of electron transfer to electron acceptor should become faster than that of back-electron transfer through careful design of PET assembly composed of a water-oxidation catalyst, photosensitizers, and electron mediator. In biocatalyzed artificial photosynthesis, the electrons provided by a donor should pass through an electron-transfer cascade by photosensitization, eventually to be used for reductive regeneration of cofactors and redox enzymatic reactions. During the journey of electrons, traps exist that interrupt the efficient flow of photoexcited electrons; for example, charge recombination and radiative/oxidative quenching,. The internal degeneration of photoexcited electrons needs to be minimized by facilitating an external electron-transport chain. For electron transfer from photosensitizer to electron mediator (e.g., **M**) for cofactor generation, a proper energy-transfer relationship between photosensitizer and electron mediator should exist, which requires a higher energy level of photoexcited electrons in the photosensitizer than the reduction potential of the electron mediator. The charge separation by electron mediator can prevent the oxidative quenching of photoexcited electrons, which causes side reactions, such as the production of superoxides and radicals by undesired acceptors (e.g., O_2).

It is also important to identify more efficient means of solar-light-harvesting. Efficient light-harvesting through the development of visible-light-active photosensitizing materials that exhibit a high quantum yield with long-term stability can enhance the efficiency and sustainability of solar-energy utilization in biocatalyzed artificial photosynthesis. Regarding the electron mediator, an Rh-based organometallic compound and its variants are among the most widely used electron mediators that can work properly by satisfying the suggested conditions for photochemical cofactor regeneration. While materials based on rare earth metals exhibit excellent performance in regioselective regeneration of cofactors, they come short of cost-efficiency and low turnover numbers. In the future, a material based on earth-abundant metals or an organic electron mediator is desired to address the current drawbacks of electron mediators. Furthermore, the integral coupling of water oxidation, electron transfer, cofactor regeneration, and biocatalysis is an ideal feature for future artificial photosynthesis. For example, the separation of reaction sites using a photoelectochemical (PEC)-type cell may provide a simple solution for overcoming the difficulty in the coupling of oxidation (i.e., water oxidation) and reduction (i.e., cofactor regeneration). In PEC cells, two electrodes, working in opposite ways toward oxidation and reduction, are connected by a wire that functions as an electron-transport chain; photoinduced water oxidation occurs in the anodic reaction site, producing protons and electrons that are transferred to the cathode for the reduction of the oxidized cofactor.

From the economic point of view, the high cost of enzyme cofactors has been prohibitive of the industrialization of many promising redox enzymatic processes. Until now, a number of different strategies for in situ regeneration of cofactors have been developed using enzymatic, chemical, electrochemical, or photochemical methods. The photochemical cofactor regeneration, a core concept in biocatalyzed artificial photosynthesis, has potential merits in the harnessing of clean and abundant solar energy, but its turnover frequencies are still low, especially in comparison with the enzymatic regeneration method; this lack of efficiency can be partly attributed to the lack of rigorous studies focused on reaction engineering and optimization. Furthermore, the long-term stability as well as cost-effectiveness of photo- and biochemical elements have not been clearly assessed yet. These issues may be addressed through the proper protection and immobilization of key reaction elements on a suitable supporting platform. Examples of redox enzymes tested for the proof of concept for biocatalytic photosynthesis only number a few thus far, but there remain many opportunities for the application of biocatalytic photosynthesis to the production of fuels and high-value chemicals, considering the variety of redox enzymatic reactions that are dependent on cofactors, such as CO_2 fixation (e.g., CO_2→formate→formaldehyde→methanol) and cytochrome P450-catalyzed reactions (e.g., O-dealkylation, deamination, and hydroxylation). Taken together, biocatalyzed artificial photosynthesis through the coupling of photocatalysis and biocatalysis is still in its infancy with many challenges remaining for further studies. The realization of biomimetic photosynthesis will require multidisciplinary efforts across the different academic fields of photochemistry, biocatalysis, materials science, and others.

Acknowledgements

This study was supported by National Research Laboratory (NRL) (2008-0060002), Converging Research Center (2010-50207), Intelligent Synthetic Biology Center of Global Frontier Project (2011-0031957), and Engineering Research Center (2012-0001175), Republic of Korea.

[1] G. W. Crabtree, N. S. Lewis, *Phys. Today* **2007**, *60*, 37–42.
[2] N. S. Lewis, D. G. Nocera, *Proc. Natl. Acad. Sci. USA* **2006**, *103*, 15729–15735.
[3] K. Sayama, K. Mukasa, R. Abe, Y. Abe, H. Arakawa, *J. Photochem. Photobiol. A* **2002**, *148*, 71–77.
[4] T. J. Meyer, *Nature* **2008**, *451*, 778–779.
[5] J. H. Alstrum-Acevedo, M. K. Brennaman, T. J. Meyer, *Inorg. Chem.* **2005**, *44*, 6802–6827.
[6] D. Gust, T. A. Moore, A. L. Moore, *Acc. Chem. Res.* **2001**, *34*, 40–48.
[7] D. Gust, T. A. Moore, A. L. Moore, *Acc. Chem. Res.* **2009**, *42*, 1890–1898.
[8] H. Imahori, Y. Mori, Y. Matano, *J. Photochem. Photobiol. C* **2003**, *4*, 51–83.
[9] H. Zhao, W. A. van der Donk, *Curr. Opin. Biotechnol.* **2003**, *14*, 583–589.
[10] J. B. van Beilen, W. A. Duetz, A. Schmid, B. Witholt, *Trends Biotechnol.* **2003**, *21*, 170–177.

[11] R. Devaux-Basseguy, A. Bergel, M. Comtat, *Enzyme Microb. Technol.* **1997**, *20*, 248–258.
[12] F. Hollmann, K. Hofstetter, A. Schmid, *Trends Biotechnol.* **2006**, *24*, 163–171.
[13] M. M. Najafpour, *Dalton Trans.* **2011**, *40*, 9076–9084.
[14] M. M. Najafpour, A. N. Moghaddam, Y. N. Yang, E. M. Aro, R. Carpentier, J. J. Eaton-Rye, C. H. Lee, S. I. Allakhverdiev, *Photosynth. Res.* **2012**, *114*, 1–13.
[15] K. N. Ferreira, T. M. Iverson, K. Maghlaoui, J. Barber, S. Iwata, *Science* **2004**, *303*, 1831–1838.
[16] H. Inoue, T. Shimada, Y. Kou, Y. Nabetani, D. Masui, S. Takagi, H. Tachibana, *ChemSusChem* **2011**, *4*, 173–179.
[17] N. D. Morris, M. Suzuki, T. E. Mallouk, *J. Phys. Chem. A* **2004**, *108*, 9115–9119.
[18] M. W. Kanan, D. G. Nocera, *Science* **2008**, *321*, 1072–1075.
[19] S. D. Tilley, M. Cornuz, K. Sivula, M. Grätzel, *Angew. Chem.* **2010**, *122*, 6549–6552; *Angew. Chem. Int. Ed.* **2010**, *49*, 6405–6408.
[20] L. Hammarström, *Curr. Opin. Chem. Biol.* **2003**, *7*, 666.
[21] I. McConnell, G. Li, G. W. Brudvig, *Chem. Biol.* **2010**, *17*, 434–447.
[22] R. Cao, W. Lai, P. Du, *Energy Environ. Sci.* **2012**, *5*, 8134–8157.
[23] A. Gabrielsson, J. R. L. Smith, R. N. Perutz, *Dalton Trans.* **2008**, 4259–4269.
[24] X. Li, M. Wang, S. Zhang, J. Pan, Y. Na, J. Liu, B. Åkermark, L. Sun, *J. Phys. Chem. B* **2008**, *112*, 8198–8202.
[25] D. R. Prasad, M. Z. Hoffman, *J. Phys. Chem.* **1984**, *88*, 5660–5665.
[26] W. Y. Teoh, J. A. Scott, R. Amal, *J. Phys. Chem. Lett.* **2012**, *3*, 629–639.
[27] Z. Goren, N. Lapidot, I. Willner, *J. Mol. Catal.* **1988**, *47*, 21–32.
[28] D. Mandler, I. Willner, *J. Chem. Soc. Chem. Commun.* **1986**, 851–853.
[29] A. Damian, S. Omanovic, *J. Mol. Catal. A* **2006**, *253*, 222–233.
[30] F. Hollmann, A. Schmid, *Biocatal. Biotransform.* **2004**, *22*, 63–88.
[31] M. M. Grau, M. Poizat, I. W. C. E. Arends, F. Hollmann, *Appl. Organomet. Chem.* **2010**, *24*, 380–385.
[32] E. Steckhan, in *Electrochemistry V, Vol. 170* (Ed.: E. Steckhan), Springer, Berlin, Heidelberg, **1994**, pp. 83–111.
[33] R. Wienkamp, E. Steckhan, *Angew. Chem.* **1983**, *95*, 508–509; *Angew. Chem. Int. Ed. Engl.* **1983**, *22*, 497–497.
[34] E. Steckhan, S. Herrmann, R. Ruppert, E. Dietz, M. Frede, E. Spika, *Organometallics* **1991**, *10*, 1568–1577.
[35] F. Hollmann, B. Witholt, A. Schmid, *J. Mol. Catal. B* **2002**, *19–20*, 167–176.
[36] F. Hollmann, I. W. C. E. Arends, K. Buehler, *ChemCatChem* **2010**, *2*, 762–782.
[37] H. C. Lo, O. Buriez, J. B. Kerr, R. H. Fish, *Angew. Chem.* **1999**, *111*, 1524–1527; *Angew. Chem. Int. Ed.* **1999**, *38*, 1429–1432.
[38] H. C. Lo, C. Leiva, O. Buriez, J. B. Kerr, M. M. Olmstead, H. Richard, *Inorg. Chem.* **2001**, *40*, 6705–6716.
[39] F. Hildebrand, C. Kohlmann, A. Franz, S. Lütz, *Adv. Synth. Catal.* **2008**, *350*, 909–918.
[40] J. Canivet, G. Süss-Fink, P. Štěpnička, *Eur. J. Inorg. Chem.* **2007**, 4736–4742.
[41] J. Barber, *Chem. Soc. Rev.* **2009**, *38*, 185–196.
[42] R. K. Yadav, J.-O. Baeg, G. H. Oh, N.-J. Park, K.-j. Kong, J. Kim, D. W. Hwang, S. K. Biswas, *J. Am. Chem. Soc.* **2012**, *134*, 11455–11461.
[43] A. Dibenedetto, P. Stufano, W. Macyk, T. Baran, C. Fragale, M. Costa, M. Aresta, *ChemSusChem* **2012**, *5*, 373–378.
[44] S. H. Lee, Y. C. Kwon, D. M. Kim, C. B. Park, *Biotechnol. Bioeng.* **2013**, *110*, 383–390.
[45] F. Hollmann, I. W. C. E. Arends, K. Buehler, A. Schallmey, B. Buhler, *Green Chem.* **2011**, *13*, 226–265.
[46] H. Jaegfeldt, *J. Electroanal. Chem.* **1981**, *128*, 355–370.
[47] P. L. Hentall, N. Flowers, T. D. H. Bugg, *Chem. Commun.* **2001**, 2098–2099.
[48] H. J. Lee, S. H. Lee, C. B. Park, K. Won, *Chem. Commun.* **2011**, *47*, 12538–12540.
[49] N. Oppenheimer in *Pyridine Nucleotide Coenzymes: Chemical, Biochemical and Medical Aspects, Part A* **1987**, p. 324.
[50] L. Rover, J. C. B. Fernandes, G. O. Neto, L. T. Kubota, E. Katekawa, S. H. P. Serrano, *Anal. Biochem.* **1998**, *260*, 50–55.
[51] A. G. Anderson, G. Berkelhammer, *J. Am. Chem. Soc.* **1958**, *80*, 992–999.
[52] S. H. Lee, H. J. Lee, K. Won, C. B. Park, *Chem. Eur. J.* **2012**, *18*, 5490–5495.
[53] V. Joosten, W. J. H. van Berkel, *Curr. Opin. Chem. Biol.* **2007**, *11*, 195–202.
[54] P. E. Garnaud, M. Koetsier, T. W. B. Ost, S. Daff, *Biochemistry* **2004**, *43*, 11035–11044.
[55] W. Van Berkel, N. Kamerbeek, M. Fraaije, *J. Biotechnol.* **2006**, *124*, 670–689.
[56] R. Ullrich, M. Hofrichter, *Cell. Mol. Life Sci.* **2007**, *64*, 271–293.
[57] A. Salimi, R. Hallaj, H. Mamkhezri, S. M. T. Hosaini, *J. Electroanal. Chem.* **2008**, *619*, 31–38.
[58] F. Hollmann, A. Taglieber, F. Schulz, M. T. Reetz, *Angew. Chem.* **2007**, *119*, 2961–2964; *Angew. Chem. Int. Ed.* **2007**, *46*, 2903–2906.
[59] A. Taglieber, F. Schulz, F. Hollmann, M. Rusek, M. T. Reetz, *ChemBioChem* **2008**, *9*, 565–572.
[60] F. E. Zilly, A. Taglieber, F. Schulz, F. Hollmann, M. T. Reetz, *Chem. Commun.* **2009**, 7152–7154.
[61] T. N. Burai, A. J. Panay, H. Zhu, T. Lian, S. Lutz, *ACS Catal.* **2012**, *2*, 667–670.
[62] E. Churakova, M. Kluge, R. Ullrich, I. Arends, M. Hofrichter, F. Hollmann, *Angew. Chem.* **2011**, *123*, 10904–10907; *Angew. Chem. Int. Ed.* **2011**, *50*, 10716–10719.
[63] M. A. Fox, *Photochem. Photobiol.* **1990**, *52*, 617–627.
[64] M. R. Wasielewski, *Chem. Rev.* **1992**, *92*, 435–461.
[65] R. Bissell, A. Prasanna de Silva, H. Q. Nimal Gunaratne, P. L. Mark Lynch, G. M. Maguire, C. McCoy, K. R. A. Samankumara Sandanayake, in *Photoinduced Electron Transfer V, Vol. 168* (Ed.: J. Mattay), Springer, Berlin, Heidelberg, **1993**, pp. 223–264.
[66] J. C. Kennedy, R. H. Pottier, *J. Photochem. Photobiol. B* **1992**, *14*, 275–292.
[67] G. A. Wagnieres, W. M. Star, B. C. Wilson, *Photochem. Photobiol.* **1998**, *68*, 603–632.
[68] B. O'Regan, M. Grätzel, *Nature* **1991**, *353*, 737–740.
[69] A. Magnuson, M. Anderlund, O. Johansson, P. Lindblad, R. Lomoth, T. Polivka, S. Ott, K. Stensjö, S. Styring, V. Sundström, L. Hammarström, *Acc. Chem. Res.* **2009**, *42*, 1899–1909.
[70] Y. Amao, *ChemCatChem* **2011**, *3*, 458–474.
[71] W. Zeng, Y. Cao, Y. Bai, Y. Wang, Y. Shi, M. Zhang, F. Wang, C. Pan, P. Wang, *Chem. Mater.* **2010**, *22*, 1915–1925.
[72] S. Fukuzumi, *Phys. Chem. Chem. Phys.* **2008**, *10*, 2283–2297.
[73] S. D. M. Islam, T. Konishi, M. Fujitsuka, O. Ito, Y. Nakamura, Y. Usui, *Photochem. Photobiol.* **2000**, *71*, 675–680.
[74] Z. Jin, X. Zhang, G. Lu, S. Li, *J. Mol. Catal. A* **2006**, *259*, 275–280.
[75] G. Ramakrishna, H. N. Ghosh, *J. Phys. Chem. B* **2001**, *105*, 7000–7008.
[76] S. Pelet, M. Grätzel, J.-E. Moser, *J. Phys. Chem. B* **2003**, *107*, 3215–3224.
[77] J. Shi, X. Zhang, D. C. Neckers, *J. Org. Chem.* **1992**, *57*, 4418–4421.
[78] S. H. Lee, D. H. Nam, J. H. Kim, J. O. Baeg, C. B. Park, *ChemBioChem* **2009**, *10*, 1621–1624.
[79] S. H. Lee, D. H. Nam, C. B. Park, *Adv. Synth. Catal.* **2009**, *351*, 2589–2594.
[80] D. H. Nam, C. B. Park, *ChemBioChem* **2012**, *13*, 1278–1282.
[81] K. Kalyanasundaram, M. Graetzel, *Curr. Opin. Biotechnol.* **2010**, *21*, 298–310.
[82] G. F. Moore, J. D. Blakemore, R. L. Milot, J. F. Hull, H. Song, L. Cai, C. A. Schmuttenmaer, R. H. Crabtree, G. W. Brudvig, *Energy Environ. Sci.* **2011**, *4*, 2389–2392.
[83] J. H. Kim, S. H. Lee, J. S. Lee, M. Lee, C. B. Park, *Chem. Commun.* **2011**, *47*, 10227–10229.
[84] A. W. Giroti, *Photochem. Photobiol.* **1983**, *38*, 745–751.
[85] G. Nahor, P. Neta, P. Hambright, A. Thompson Jr, A. Harriman, *J. Phys. Chem.* **1989**, *93*, 6181–6187.
[86] H. Asada, T. Itoh, Y. Kodera, A. Matsushima, M. Hiroto, H. Nishimura, Y. Inada, *Biotechnol. Bioeng.* **2001**, *76*, 86–90.

[87] F. M. Toma, A. Sartorel, M. Iurlo, M. Carraro, P. Parisse, C. Maccato, S. Rapino, B. R. Gonzalez, H. Amenitsch, T. Da Ros, *Nat. Chem.* **2010**, *2*, 826–831.
[88] S. Choudhury, J. O. Baeg, N. J. Park, R. K. Yadav, *Angew. Chem.* **2012**, *124*, 11792–11796; *Angew. Chem. Int. Ed.* **2012**, *51*, 11624–11628.
[89] K. Maeda, K. Domen, *J. Phys. Chem. Lett.* **2010**, *1*, 2655–2661.
[90] R. Abe, *J. Photochem. Photobiol. C* **2010**, *11*, 179–209.
[91] A. Kudo, Y. Miseki, *Chem. Soc. Rev.* **2009**, *38*, 253–278.
[92] Z. Jiang, C. Lü, H. Wu, *Ind. Eng. Chem. Res.* **2005**, *44*, 4165–4170.
[93] D. Chen, D. Yang, Q. Wang, Z. Jiang, *Ind. Eng. Chem. Res.* **2006**, *45*, 4110–4116.
[94] Q. Shi, D. Yang, Z. Jiang, J. Li, *J. Mol. Catal. B* **2006**, *43*, 44–48.
[95] C. B. Park, S. H. Lee, E. Subramanian, B. B. Kale, S. M. Lee, J. O. Baeg, *Chem. Commun.* **2008**, 5423–5425.
[96] S. S. Bhoware, K. Y. Kim, J. A. Kim, Q. Wu, J. Kim, *J. Phys. Chem. C* **2011**, *115*, 2553–2557.
[97] A. Van Dijken, J. Makkinje, A. Meijerink, *J. Lumin.* **2001**, *92*, 323–328.
[98] D. H. Nam, S. H. Lee, C. B. Park, *Small* **2010**, *6*, 922–926.
[99] S. H. Lee, J. Ryu, D. H. Nam, C. B. Park, *Chem. Commun.* **2011**, *47*, 4643–4645.
[100] J. Ryu, S. H. Lee, D. H. Nam, C. B. Park, *Adv. Mater.* **2011**, *23*, 1883–1888.
[101] H. Zhang, G. Chen, D. W. Bahnemann, *J. Mater. Chem.* **2009**, *19*, 5089–5121.
[102] E. Garnett, P. Yang, *Nano Lett.* **2010**, *10*, 1082–1087.
[103] I. Oh, J. Kye, S. Hwang, *Nano Lett.* **2012**, *12*, 298–302.
[104] Y. Cui, Z. Zhong, D. Wang, W. U. Wang, C. M. Lieber, *Nano Lett.* **2003**, *3*, 149–152.
[105] H. Y. Lee, J. Ryu, J. H. Kim, S. H. Lee, C. B. Park, *ChemSusChem* **2012**, *5*, 2129–2132.
[106] P. D. Frischmann, K. Mahata, F. Würthner, *Chem. Soc. Rev.* **2013**, *42*, 1847–1870.
[107] D. Noy, *Photosynth. Res.* **2007**, *95*, 23–35.
[108] J. Barber, B. Andersson, *Nature* **1994**, *370*, 31–34.
[109] W. F. J. Vermaas, S. Styring, W. P. Schröder, B. Andersson, *Photosynth. Res.* **1993**, *38*, 249–263.
[110] E. S. Andreiadis, M. Chavarot-Kerlidou, M. Fontecave, V. Artero, *Photochem. Photobiol.* **2011**, *87*, 946–964.
[111] K. V. Rao, K. Datta, M. Eswaramoorthy, S. J. George, *Chem. Eur. J.* **2012**, *18*, 2184–2194.
[112] Y. S. Nam, A. P. Magyar, D. Lee, J. W. Kim, D. S. Yun, H. Park, T. S. Pollom, D. A. Weitz, A. M. Belcher, *Nat. Nanotechnol.* **2010**, *5*, 340–344.
[113] K. Maeda, M. Eguchi, S.-H. A. Lee, W. J. Youngblood, H. Hata, T. E. Mallouk, *J. Phys. Chem. C* **2009**, *113*, 7962–7969.
[114] J. C. Rooke, C. Meunier, A. Léonard, B. L. Su, *Pure Appl. Chem.* **2008**, *80*, 2345–2376.
[115] S. L. Jain, J. K. Joseph, F. E. Kühn, O. Reiser, *Adv. Synth. Catal.* **2009**, *351*, 230–234.
[116] T. T. Teeri, H. Brumer, G. Daniel, P. Gatenholm, *Trends Biotechnol.* **2007**, *25*, 299–306.
[117] M. Lee, J. H. Kim, S. H. Lee, S. H. Lee, C. B. Park, *ChemSusChem* **2011**, *4*, 581–586.
[118] E. Adler, *Wood Sci. Technol.* **1977**, *11*, 169–218.
[119] G. Milczarek, *Electroanalysis* **2007**, *19*, 1411–1414.
[120] P. Jordan, P. Fromme, H. T. Witt, O. Klukas, W. Saenger, N. Krauß, *Nature* **2001**, *411*, 909–917.
[121] M. R. Wasielewski, *Acc. Chem. Res.* **2009**, *42*, 1910–1921.
[122] J. H. Kim, M. Lee, J. S. Lee, C. B. Park, *Angew. Chem.* **2012**, *124*, 532–535; *Angew. Chem. Int. Ed.* **2012**, *51*, 517–520.
[123] J. S. Lee, S. H. Lee, J. H. Kim, C. B. Park, *Lab Chip* **2011**, *11*, 2309–2311.
[124] R. O. Loutfy, J. H. Sharp, *Photogr. Sci. Eng.* **1976**, *20*, 165–174.
[125] K. Kalyanasundaram, M. Neumann-Spallart, *J. Phys. Chem.* **1982**, *86*, 5163–5169.
[126] C. Grimes, O. Varghese, S. Ranjan, *Light, Water, Hydrogen: The Solar Generation of Hydrogen by Water Photoelectrolysis*, Springer, New York, **2007**, pp. 115–190.

Published online: February 21, 2013

